

Control of wire transfer behaviors in hot wire laser welding

Wen Peng^{1,2} · Shan Jiguo¹ · Zheng Shiqing¹ · Wang Gang^{1,2}

Received: 9 June 2015 / Accepted: 3 August 2015 / Published online: 27 August 2015
© Springer-Verlag London 2015

Abstract Hot wire laser welding reduces the requirement of wire feeding accuracy and improves wire deposition efficiency with preheating wire by resistance heat. Due to merits like low heat input and high deposition rate, this method has broad potential applications like welding and additive manufacturing. It is a key problem to maintain stable wire transfer in hot wire laser welding since the preheated wire should be kept contacted with the work piece to maintain high temperature. A high-speed imaging system was used to observe wire transfer behaviors, which are divided into three types: fusing transfer, continuous transfer, and wire hit transfer. Only the continuous transfer is the stable wire transfer, which guarantees good weld formation. The wire transfer behavior is determined by wire temperature, and the temperature criterion of wire transfer is obtained by image analysis and temperature measurement. Two characteristic points P1 and P2 on the filler wire were found out, whose temperatures were used to judge wire transfer behaviors. The temperature criterion of the stable wire transfer is interpreted that the temperature of P1 (T_{P1}) must be no more than the wire solidus and the temperature of P2 (T_{P2}) must be no less than the wire liquidus. A heat conduction model of hot wire laser welding was established to calculate T_{P1} and T_{P2} for the used 308-L stainless wire. The welding

parameters, which made up isothermal surfaces of $T_{P1}=1398$ °C and $T_{P2}=1454$ °C, respectively, the solidus and liquidus of the used wire, were obtained by iteration calculation of wire temperature. The parameters window of the stable wire transfer was located between the two isothermal surfaces. For the stable wire transfer in hot wire laser welding, the resistance heat of the wire cannot exceed the heat which fuses the wire tip outside the molten pool. Meanwhile, the total heat of the wire, including the resistance heat and the heat conducted from the molten pool, must exceed the heat which melts the wire tip inside the molten pool.

Keywords Laser welding · Laser cladding · Hot wire · Numerical simulation · High-speed imaging

1 Introduction

Laser is regarded as an advantaged heat source for welding and cladding due to its low heat input, accurate heating, low distortion, and high flexibility, etc. Traditional laser welding usually does not use filler wire, considering two main problems: poor wire transfer stability and low deposition efficiency. The problems can be explained by the high requirements to feed wire accurately into the focused laser spot and to melt wire and base metal at the same time [1]. Laser welding is limited in many application fields without filler wire, such as welding plates with large gap or heavy thickness, and welding materials necessary to adjust chemical compositions of weld metal [2, 3]. In hot wire laser welding, double heat sources including laser energy and resistance heat are used to heat base metal and filler wire independently. The preheated wire reduces the demands of strict wire positioning and high laser power. Moreover, both high deposition efficiency and small heat damage to base metal can be obtained meanwhile.

Electronic supplementary material The online version of this article (doi:10.1007/s00170-015-7696-8) contains supplementary material, which is available to authorized users.

✉ Wen Peng
wenpeng@tsinghua.edu.cn

¹ The State Key Laboratory of Tribology, Tsinghua University, Beijing 100084, China

² Department of Mechanical Engineering, Tsinghua University, Beijing 100084, China

Thus, with filling hot wire, the application of laser welding is enlarged, especially suitable for cladding [4–7] and narrow gap welding [8, 9]. Moreover, laser welding with filling hot wire can be developed as a method for laser additive manufacturing with unique merits of low heat input and high deposition efficiency.

There have been some reports on the merits of hot wire laser welding. Nurminen et al. compared the formation quality and efficiency between powder, cold wire, and hot wire in laser cladding [4, 5]. They found that hot wire laser cladding showed the lowest dilution and the highest deposition rate and concluded that the low heat damage to substrate by using hot wire can bring in many merits in practical applications. Wen et al. used hot wire laser cladding to repair martensitic stainless steel. The repaired formation quality was quite good, and the dilution ration was as lows as less than 10 % [7]. Katayama et al. used cold and hot wire to weld 590 MPa steel by laser. Formation defects like collapse and burn-through of the molten pool were easily found by cold wire, while a wide processing window with good formation quality was obtained by hot wire [8]. Shinozaki et al. developed narrow gap hot wire laser welding to join high-strength steels, Ni alloys, and 9Cr steels [9]. The mechanical test on hot wire laser welded joints shows comprehensive advantages over other welding methods. Jones et al. found that hot wire laser welding can prevent hot cracking in nickel-based alloys [10].

During hot wire laser welding, the galvanic wire tip touches base metal so that resistance heat preheats wire to certain temperature. The preheated wire was fed into the molten pool and needs a little conduction heat from the pool to melt. Thus, in order to maintain stable wire transfer, it is a critical issue to choose filling wire speed and current to maintain appropriate preheat temperature and choose laser heat input to melt the wire. Shinozaki et al. experimentally investigated the influence of welding parameters, such as laser spot diameter, current, laser-wire distance, wire feeding rate on weld formation for the narrow gap joint [9], lap joint [11], and fillet joint [12]. Dr. Kovacevic et al. did experimental and numerical research work on laser hot wire welding [6, 13, 14]. They used real-time monitoring to investigate wire transfer behavior, especially the effect of the applied voltage. The electron temperature was used as an indicator of the instability of the process and weld quality. The above reports all consider that it is a key factor to keep the wire feeding into the molten pool stably in order to obtain good weld formation. Only the stable wire transfer can obtain good weld formation. However, welding parameters have combined and complex influence on wire transfer behaviors. The previous researches all selected welding parameters by trial and error. It is theoretically not clear so far how to obtain the proper welding parameters for the stable wire transfer.

In this paper, hot wire transfer behaviors were observed and categorized by high-speed imaging method. Two

characteristic points P1 and P2 on the filler wire were found out, and their temperatures were concluded as the criterions of wire transfer behaviors. Numerical model was established to calculate hot wire temperature. Finally, the parameters window and control principle of the stable wire transfer is concluded for hot wire laser welding.

2 Experimental materials and methods

Base metal is a 3-mm mild steel plate. Filler wire is a 308-L austenite stainless steel with 1.2 mm diameter. The solidus of the filler wire is 1398 °C, and the liquidus is 1454 °C. The chemical compositions of base metal and the filler wire are shown in Table 1.

Figure 1 shows the setup of hot wire laser welding equipment. An IPG fiber laser was used with wavelength 1.07 μm to weld the plate. A Panasonic constant current power source was used to preheat filler wire. The positive pole was connected with wire by the copper tube and the negative with base metal. If the wire touched base metal, a circuit formed and the wire was heated. The preheated wire fed into the trailing edge of the molten pool without direct irradiation of laser beam and melted with the heat from the molten pool. The A Photron SA3 high-speed camera was used to observe the wire transfer behaviors. The frame rate was 250 f/s; the shutter time was 1/6000 s. A semiconductor laser with 8.8 W power and 810 nm wavelength provided lightening for high-speed imaging. A Raytek MR1SCSF infrared ratio thermometer was used to measure the temperature of the wire outside the molten pool. The measurement range was 1000–3000 °C; the accuracy was ± 15 °C; the spectrometer was 0.75–1.1 μm ; the sampling frequency was 20 Hz; the response time was 10 ms.

To find out the influence of laser energy and resistance heat on wire transfer behaviors, laser power (P), current (I), and wire feeding rate (V_f) were changed as variables. The range was set as follows: 1–2 kW for laser power, 0–120 A for wire current, and 1–3 m/min for wire feeding rate. Other welding parameters were chosen by preliminary experiments and kept constant: 0.5 m/min for welding speed, 3 mm for laser spot diameter, 1 mm for the initial distance from laser spot to the wire, 70° for wire feeding angle, and 35 mm for the initial wire length.

The wire keeps moving and stays at high temperature, so the temperature measurement of hot wire tip has been regarded formidable in laser welding, especially considering

Table 1 Chemical compositions of base metal and filler wire

Wt (%)	C	Si	Mn	Cr	Ni	Fe
Base metal	0.18	0.30	0.50	–	–	Bal
Filler wire	0.024	0.42	1.65	20.1	10.33	Bal

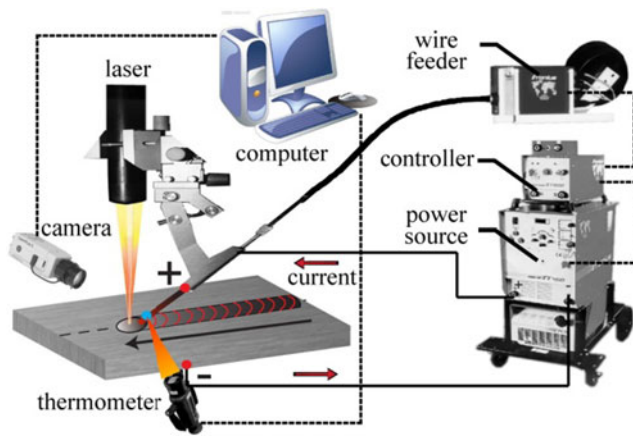


Fig. 1 Experimental system of hot wire laser welding

that the wire tip is so close to the molten pool. Since the wavelength of the fiber laser lies within the spectrometer of the infrared ratio thermometer, laser reflection and metal vapor are absorbed by the thermometer and make the measurement overflow in normal condition. Pulsed laser was used for temperature measurement to prevent the disturbance. Figure 2 shows the measurement results of the wire tip outside the molten pool with pulsed laser. The measurement position is located at the wire 30 mm away from the contact point, represented by T_{30} . The measurement becomes unsteady if the measurement point is much closer to the molten pool. The peak power is 2 kW, the pulsed cycle is 1 s, and the duty ratio is 90 %. When the laser is on, the temperature overflows due to the absorption of the strong reflected laser; when laser is off, the wire temperature is measured.

The influence of peak power and duty ratio on the wire temperature is investigated as Fig. 3 shows. The measurement position is as the same as that in Fig. 2. The maximum difference among the measured temperatures is 14 °C, which is smaller than the measurement accuracy ± 15 °C. It means that the change of laser power has little influence on the temperature of wire tip. Thus, it is reasonable and effective to use pulsed laser rather than continuous laser for temperature measurement of the hot wire tip outside the molten pool.

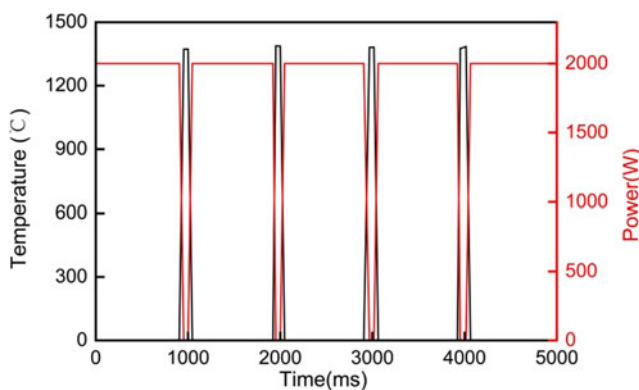


Fig. 2 Temperature measurement of the wire tip with pulsed laser: ($V_f=2$ m/min, $I=95$ A, cycle=1 s, duty ratio=90 %)

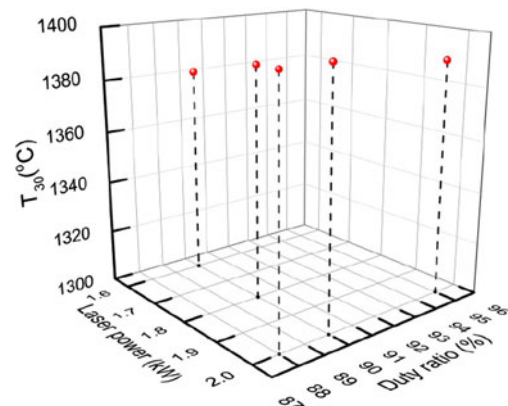


Fig. 3 Effect of peak power and duty ratio on wire temperature with pulsed laser: ($I=95$ A, $V_f=2$ m/min, cycle=1 s)

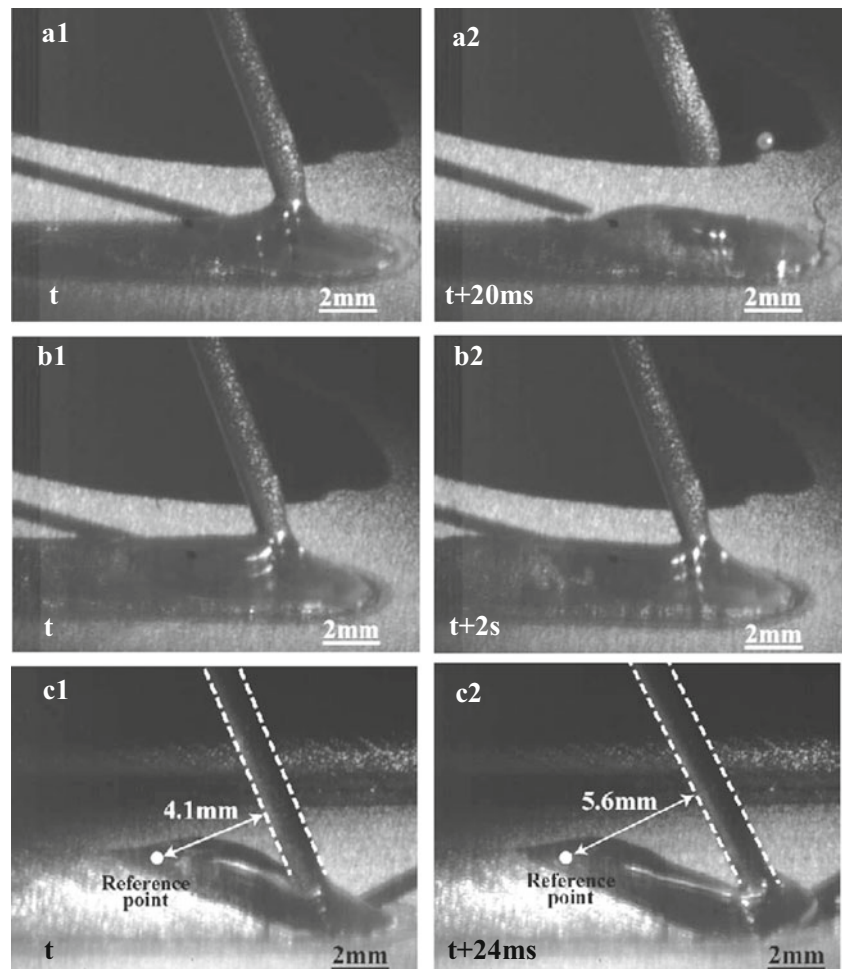
3 Result and analysis

3.1 Classification of wire transfer behaviors and their influence on weld formation

Wire transfer behaviors under different welding parameters were observed by the high-speed camera during hot wire laser welding. It is found that welding parameters have obvious influence on wire transfer behaviors. The change of wire transfer behaviors with the current is shown in Fig. 4. The adjusting step of current is 5 A. When the current is too high (Fig. 4a, $I \geq 100$ A), the wire tip fuses and gets out of touch of the molten pool. Then, the wire is fed into the molten pool again. This type of wire transfer behavior is named as fusing transfer. When the current is medium (Fig. 4b, $55 \text{ A} \leq I \leq 95 \text{ A}$), the wire keeps stably melting in the molten pool. It is named as continuous transfer. The melted volume of wire keeps constant in the molten pool, so the continuous transfer is regarded as the stable wire transfer. When the current is too low (Fig. 4c, $I \leq 50$ A), the wire cannot melt timely and hits the bottom of the molten pool. From high-speed images, the swing of wire tip can be clearly observed. The distance from the wire to a fixed reference point changes in the welding process in Fig. 4c. It is considered that the hitting impact causes the wire to swing frequently back and forth in the molten pool. This type of wire transfer behavior is named as wire hit transfer.

Wire feeding rate and laser power also have influence on wire transfer behaviors according to experiments. Low wire feeding rate usually results in the fusing transfer; high wire feeding rate and low laser power usually result in the wire hit transfer. Medium wire feeding rate and high enough laser power are easily used to obtain the continuous transfer. However, it should be noted that the fusing transfer is possibly resulted by excessive laser heat input unless in a much large offset distance, since the strong radiation heat of laser beam will enhance the melting of hot wire tip outside the molten pool.

Fig. 4 High-speed images of wire transfer behaviors: **a** $I=120$ A; **b** $I=90$ A; and **c** $I=20$ A: ($P=2$ kW, $V_f=2$ m/min)



Wire transfer behaviors have obvious influence on weld formation quality. The fusing transfer causes spatters and a discontinuous weld, as shown in Fig. 5a. The wire hit transfer results in a warping weld, as shown in Fig. 5c. Only the continuous transfer, namely the stable wire transfer, obtains good weld formation, as shown in Fig. 5b. Therefore, the bead formation is determined by wire transfer behaviors for single pass bead-on plate welding. The continuous transfer is necessary for good weld formation in hot wire laser welding.



Fig. 5 Typical weld formation under different wire transfer types: **a** 120 A; **b** 90 A; and **c** 20 A: ($P=2$ kW, $V_f=2$ m/min)

3.2 Criteria of wire transfer behaviors

By analyzing high-speed images, the three types of wire transfer behaviors are concluded and illustrated in Fig. 6. The letter F means the melting position in wire. For the fusing transfer (Fig. 6a), the wire melts at F_2 in the molten pool at first. After a moment, the wire obtains so much resistance heat that it fuses at F_1 outside the pool. For the continuous transfer (Fig. 6b), the preheated wire absorbs conduction heat from the molten pool and it keeps stably melting at F in the pool. For the wire hit transfer (Fig. 6c), the preheated wire cannot melt in time, and hit the bottom of the molten pool. The hitting delays wire filling rate, so the wire can absorb more heat from the pool. In the worst condition, the wire cannot melt in the pool and the wire feeding is broken off. Thus, the difference among the three wire transfer types lies in the melting position of hot wire, which is certainly dependent on the wire temperature. Thus, the wire temperature can be used as the criterion of wire transfer behaviors.

Partial melting is found at the wire tip outside the molten pool for some welding conditions with the continuous transfer by high-speed imaging. Figure 7 shows the influence of

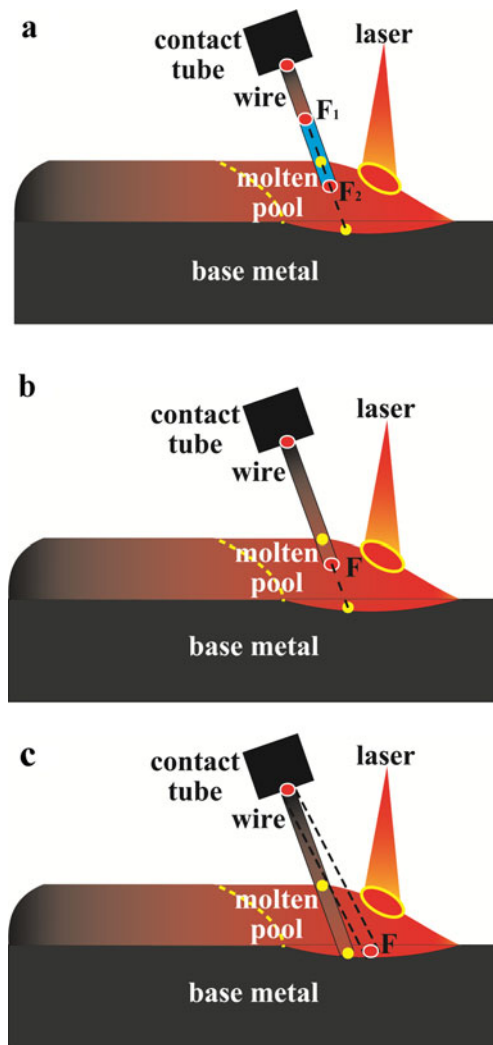


Fig. 6 Illustration of wire transfer behaviors: **a** fusing transfer; **b** continuous transfer; and **c** wire hit transfer

current on the partial melting length of the wire tip (named as L_{PM}) with $V_f=2$ m/min. The L_{PM} increases from 0 to 3 mm when the current increases from 80 to 95 A (Fig. 7a–c). For 95 A, the solid wire outside the molten pool starts melting at the point 5 mm away from the surface of the pool, namely 30 mm away from the contact tube. Once the current increases to 100 A, the L_{PM} will exceed 3 mm. In this condition, the stiffness of the wire tip becomes so low that it cannot resist necking down caused by the electromagnetic contraction force. The wire begins fusing outside the molten pool, namely changing into the fusing transfer (Fig. 7d). Thus, when the current is 95 A, the wire transfer behavior is considered as the critical status between the continuous and the fusing transfer, and the L_{PM} is named as the critical L_{PM} (named as L_{CPM}). When the current is increased further, partial melting cannot be maintained, and the wire transfer behavior changes to the fusing transfer. Based on the above analysis, the wire position from which the distance to the molten pool equals to the L_{CPM}

is defined as the characteristic point 1 (P1). Its temperature (T_{P1}) can be the criterion of the fusing transfer. If T_{P1} exceeds the wire solidus, meaning that partial melting length is over L_{CPM} , the wire transfer behavior is the fusing transfer. According to Fig. 7c, P1 is located at 30 mm away from the contact tube, and L_{CPM} is 3 mm for the used wire.

T_{30} is measured as 1395 °C by the infrared ratio thermometer under the critical status with $I=95$ A and $V_f=2$ m/min as shown in Fig. 2, which is very close to the solidus of the used 1398 °C wire. It verifies the observation results from high-speed images. When L_{PM} is 3 mm, the wire transfer behavior is in the critical status between the continuous and fusing transfer. If the wire absorbs more heat, T_{30} will exceed the solidus temperature, and the L_{PM} will be over 3 mm. Therefore, with locating the position of P1, the fusing transfer can be predicted by the temperature criterion: if T_{P1} is higher than the wire solidus ($T_{30} \geq 1398$ °C for the used wire), it is fusing transfer.

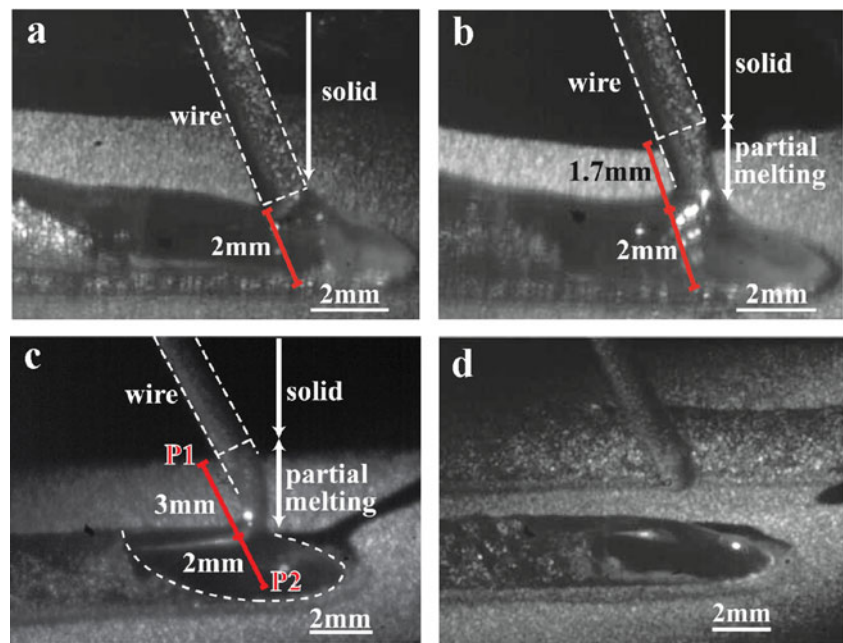
There are two heat sources for hot wire: laser energy and resistance heat. For the wire outside the molten pool, laser power has little influence on the wire temperature according to Fig. 3, which means that the position of P1 has nothing to do with laser energy. In fact, the L_{CPM} represents the stiffness of the wire tip at high temperature, so the position of P1 is only decided by chemical composition and geometry of the used wire. Figure 8 shows the high-speed image of L_{CPM} under different wire feeding rate. The current is chosen at the critical status between continuous and fusing transfer. The partial melting length outside the molten pool is just as the same as 3 mm, and T_{30} is also measured very close to the solidus 1398 °C.

The point at the end of the wire, which contacts with the bottom of the molten pool, is defined as the characteristic point 2 (P2). Obviously, its temperature (T_{P2}) can be the criterion of the wire hit transfer. If T_{P2} is below the wire liquidus, the wire end will show some stiffness and hit the bottom of the molten pool. The distance from P2 to the contact tube is shown in Eq. (1). S_L is the distance from P2 to the contact tube, L is the initial wire length, h is the depth of the molten pool, and α is the wire feeding angle. The position of P2 is mainly decided by the initial wire length and the depth of molten pool. Defocused laser with spot diameter as 3 mm is used, and the laser power is lower than 2 kW in this paper. It is found that the depth of the molten pool is so small that it can be ignored. It means that the distance from P2 to the contact tube can be regarded approximately to the wire initial length 35 mm.

$$S_L = L + h/\cos\alpha \quad (1)$$

With locating the position of P2, the wire hit transfer can be predicted by the temperature criterion: if T_{P2} is lower than the wire liquidus ($T_{35} \leq 1454$ °C for the used wire), it is wire hit

Fig. 7 Influence of current on L_{PM} : **a** 80 A; **b** 90 A; **c** 95 A; and **d** 100 A; ($P=2$ kW, $V_f=2$ m/min)



transfer. Therefore, the continuous transfer can be predicted by the criterion: T_{P1} is lower than the wire solidus; T_{P2} is higher than the wire liquidus ($T_{30} \leq 1398$ °C and $T_{35} \geq 1454$ °C for the used wire). Since only the continuous transfer can guarantee that the wire melts stably in the molten pool, the welding parameters should be chosen so that T_{P1} and T_{P2} meet with the temperature criterion of the continuous transfer.

3.3 Numerical simulation and verification of wire temperature

Numerical simulation is used to calculate T_{P1} and T_{P2} . The geometry size of the numerical model is shown in Fig. 9. The size of base metal is 120 mm×60 mm×3 mm. The wire diameter is 1.2 mm, and the initial length is set as 35 mm. It is found that the bead shape is mainly related to the volume of feeding wire. When the wire feeding rate is 2 m/min, the height and width of deposited weld metal are respectively set as 1.75 and 3.5 mm based on the cross section of the practical bead. The length of the molten pool in front of the wire is set as 2.5 mm based on high-speed images. If the wire

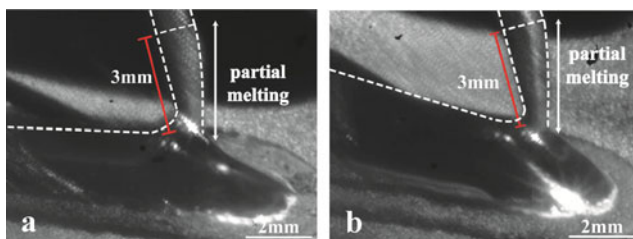


Fig. 8 L_{PMI} under different wire feeding rates: **a** 1 m/min, 67 A and **b** 3 m/min, 116 A; ($P=2$ kW)

feeding rate changed, the size of the numerical model should be revised based on the bead shape.

Both the temperature of wire and base metal can be obtained by the differential equation of heat conduction as shown in Eq. (2). The heat sources on wire include three parts mainly: resistance heat, conduction heat from the molten pool, and radiation heat from laser reflection and the molten pool. The resistance heat is calculated by Joule's law, as shown in Eq. (3). The conduction heat is related to the temperature of the molten pool. Since a defocused low power laser was used, the penetration depth was very shallow according to experimental observation, like the shape created by arc heat. Therefore, the laser heat source imposed on base metal is expressed by the double ellipsoid heat model as shown in Eqs. (4). Equation (5) shows the motion of laser heat source controlled by welding speed. The radiation heat from laser reflection and the molten pool is calculated by a Gaussian hemisphere heat model as shown in Eq. (6). With increasing the distance from the

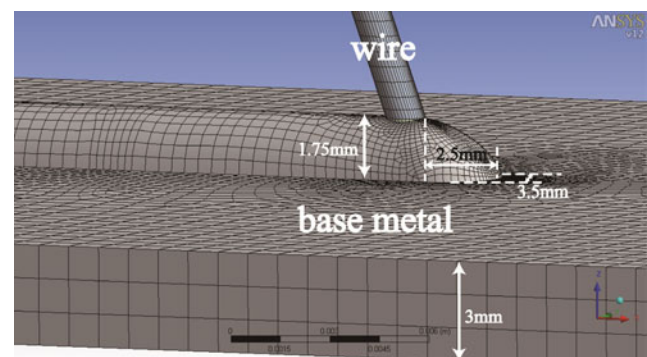


Fig. 9 Geometry size of model of wire temperature field

surface of the molten pool, the radiation energy drops down quickly on the wire tip outside the molten pool.

Conduction heat from the molten pool to the wire is expressed by the coupling heat transfer boundary condition. The temperature and heat flux are continuous at the interface between the wire and the molten pool. Heat dissipation of the wire and molten pool to the environment is expressed by the third boundary condition in Eq. (7). The wire temperature can be calculated by solving Eqs. (2)–(7).

$$\frac{\partial T}{\partial t} = \frac{\lambda}{\rho c} \left(\frac{\partial^2 T}{\partial x^2} + \frac{\partial^2 T}{\partial y^2} + \frac{\partial^2 T}{\partial z^2} \right) + \frac{\Phi}{\rho c} \quad (2)$$

$$q_R = \frac{I^2 R}{dV} = \frac{I^2 \cdot \rho' \cdot dl}{S \cdot dl} = \frac{I^2 \cdot \rho'}{S^2} \quad (z > 1.75) \quad (3)$$

$$q_f = \frac{6\sqrt{3}f_f P}{\pi^3/2 a_f b_f c_f} \exp\left(-3\left(\left(\frac{x}{a_f}\right)^2 + \left(\frac{y}{b_f}\right)^2 + \left(\frac{z}{c_f}\right)^2\right)\right)^{(x>0)}$$

$$q_r = \frac{6\sqrt{3}f_r P}{\pi^3/2 a_r b_r c_r} \exp\left(-3\left(\left(\frac{x}{a_r}\right)^2 + \left(\frac{y}{b_r}\right)^2 + \left(\frac{z}{c_r}\right)^2\right)\right)^{(x<0)} \quad (4)$$

$$q_m = -\frac{\partial(\rho_b h_b u_x)}{\partial x} \quad (5)$$

$$q_F(x, y, z) = \frac{P_r}{\pi \cdot \sqrt{\pi} \cdot r^3} \cdot \exp\left(3 \frac{x^2 + y^2 + z^2}{r^2}\right) \quad (z > 1.75) \quad (6)$$

$$\lambda \frac{\partial T}{\partial n} = h(T_C - T_W) \quad (7)$$

In Eq. (2), T : temperature of wire or base metal, t : time, λ : heat conductivity of wire or base metal, ρ : density of wire or base metal, c : specific heat of wire or base metal, and Φ : heat source of wire or base metal. In Eq. (3), q_R : heat flux of resistance heat, I : wire current, R : wire resistance, dV : infinitesimal volume, S : cross section area of wire, ρ' : wire resistivity, and dl : infinitesimal length. In Eq. (4), P : laser power, q_f : heat flux of the front hemi-ellipsoid, and q_r : heat flux of the back hemi-ellipsoid. The notation a_f , b_f , and c_f are respectively the length of the semi-axes in x , y , z direction; f_f and f_r are respectively the coefficients of the front and back hemi-ellipsoid. The sum of f_f and f_r equals to the value of 2. In Eq. (5), ρ_b : density of base metal, h_b : enthalpy of base metal, and u_x : welding speed. In Eq. (7), h : surface heat transfer coefficient, T_C : surrounding temperature, and T_W : wire temperature.

The temperature distribution of wire outside the molten pool is shown in Fig. 10. The wire temperature increases almost linearly along the length direction of the wire. The closer to the molten pool, the higher the temperature is. With increasing current, the wire temperature increases. For current 95 A, different points are measured along the wire. T_{30} were also

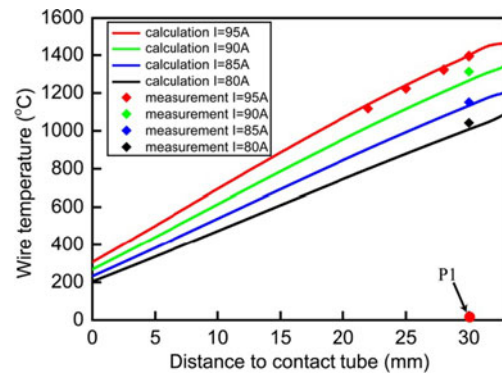


Fig. 10 Comparison of T_{P1} between calculation and measurement; ($P=2$ kW, $V_f=2$ m/min)

measured under different currents. The calculated values are very close to the measured values. The temperature of point 30 mm away from the contact point A (T_{30}) is 1395 °C for current 95 A, which approaches to the solidus temperature of wire. The results indicate that the calculated temperature fields of the wire part outside the molten pool are credible.

3.4 Control of stable wire transfer

Figure 11 shows the calculated temperature contour of the wire part near and inside the molten pool under current 100, 90, and 50 A. Laser power and wire feeding rate are fixed as 2 kW and 2 m/min. When the current is 100 A, $T_{30}=1510$ °C, higher than the solidus 1398 °C. The wire transfer behavior is predicted as the fusing transfer. When the current is 50 A, $T_{35}=1402$ °C, lower than the liquidus 1454 °C, which means the wire hit transfer. When the current is 90 A, $T_{30}=1302$ °C and $T_{35}=1742$ °C. The wire transfer is predicted as the stable wire transfer. The prediction results are confirmed by the images captured by high-speed camera. Therefore, by comparing the calculated wire temperature with the temperature criterions of wire transfer behaviors, wire transfer behaviors under various welding parameters can be predicted. Moreover, the parameters window of the stable wire transfer can be predicted as well with calculating out the parameters under the critical conditions of wire transfer behaviors.

Current, wire feeding rate and laser power are chosen as the variable parameters, others are kept constant among all the input parameters. The variable parameters are iterated programmatically to calculate T_{P1} and T_{P2} , until the two temperatures gets approximately to the wire solidus 1398 °C and liquidus 1454 °C, respectively. First of all, an initial current is selected randomly for certain wire feeding rate with $P=2$ kW. T_{P1} are calculated with different wire feeding rates and currents and shown as red dots in Fig. 12. If the calculated T_{P1} is higher than 1398 °C, the current is decreased to calculate T_{P1} again; or else, the current is increased until T_{P1} gets to 1398 °C. By self-adaptively adjusting current, different parameter points with wire feeding rate, which makes T_{P1} equal

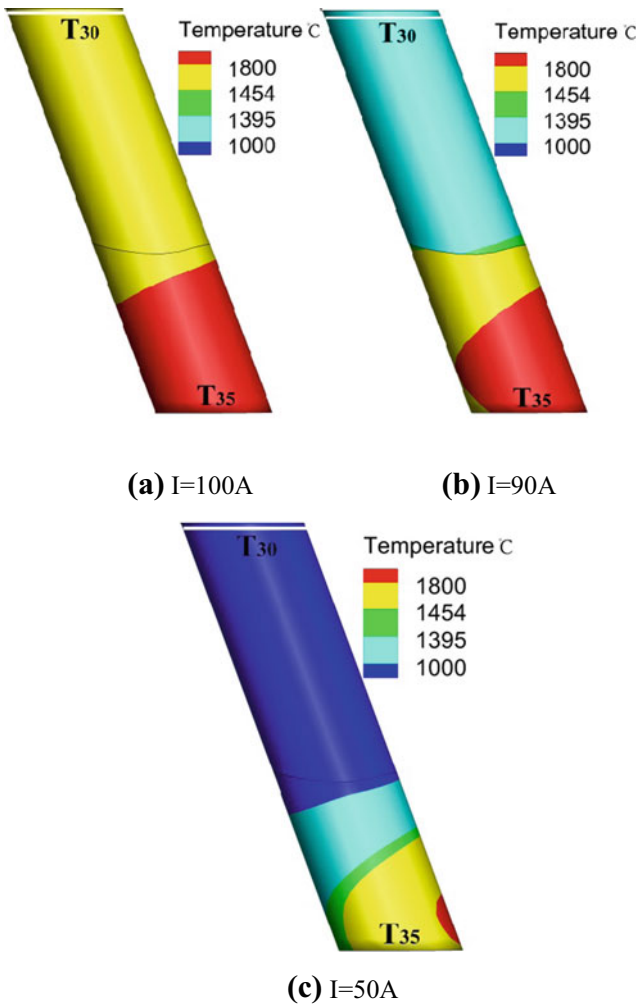


Fig. 11 a–c Calculated wire temperature near and inside the molten pool

to 1398 °C, are obtained. The isothermal line of $T_{P1}=1398$ °C is obtained and shown as the curve in Fig. 12 by joining these points. Similarly, the isothermal line of $T_{P1}=1398$ °C is

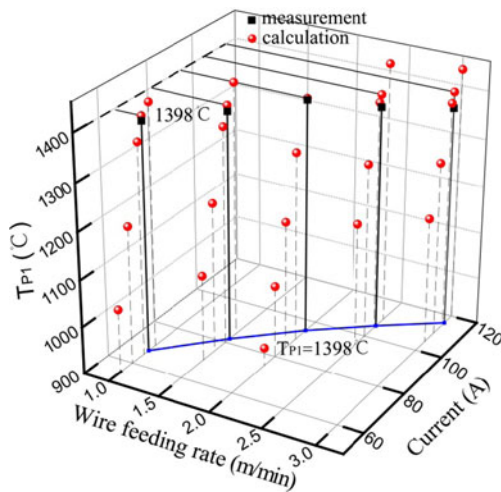


Fig. 12 Influence of wire feeding rate and current on calculated T_{P1} ; ($P=2$ kW)

obtained under different power with keeping wire feeding rate as constant as $V_f=2$ m/min and is shown in Fig. 13. The isothermal line is parallel to the axis of laser power, which means that T_{P1} is not affected by laser power.

The temperatures of five points on the isothermal line are measured and the results are shown as black squares in Fig. 12. The maximum difference between the calculated and measured values is 33 °C, which is acceptable considering the accuracy of the infrared ratio thermometer. Besides, welding experiments are done with currents near the isothermal line under various wire feeding rates. It is confirmed experimentally that the stable wire transfer is obtained with current in the isothermal line, and the fusing transfer is obtained with current 5 A over the value in the isothermal line. Therefore, the fusing wire transfer can be predicted if the current is over the isothermal line for certain wire feeding rate.

Likewise, the isothermal line of $T_{P2}=1454$ °C is searched and shown in Fig. 14 with $P=2$ kW. T_{P2} are calculated out under various wire feeding rates and currents and shown as red circles. By joining points with $T_{P2}=1454$ °C, the isothermal line is obtained and shown in Fig. 14. The isothermal lines of $T_{P2}=1454$ °C are also obtained with $P=1.8$ kW, $P=1.6$ kW, and $P=1.2$ kW, respectively, as shown in Fig. 15. The isothermal line moves up with decreasing laser power. It is confirmed experimentally that the stable wire transfer is obtained with current in the isothermal line, and the wire hit transfer is obtained with current 5 A less than the value in the isothermal line. Therefore, for certain wire feeding rate, the wire hit transfer can be predicted if the current is below the isothermal line.

So far, the isothermal surface of $T_{P1}=1398$ °C and $T_{P2}=1454$ °C can be obtained in Fig. 16 with current, wire feeding rate, and laser power as the variables. The upper surface is the isothermal surface of $T_{P1}=1398$ °C. If the welding parameters in the isothermal surface are chosen, the critical status of stable wire transfer is obtained. If the welding parameters over the

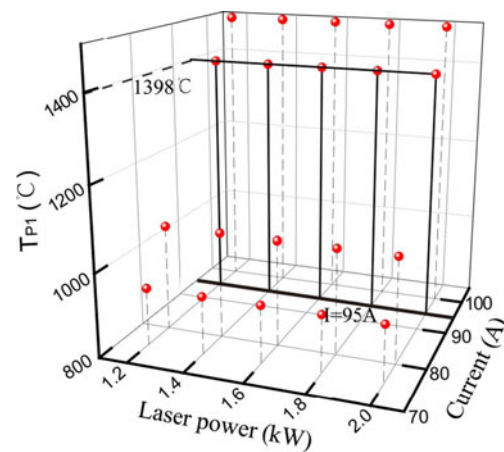


Fig. 13 Influence of laser power and current on the calculated T_{P1} ; ($V_f=2$ m/min)

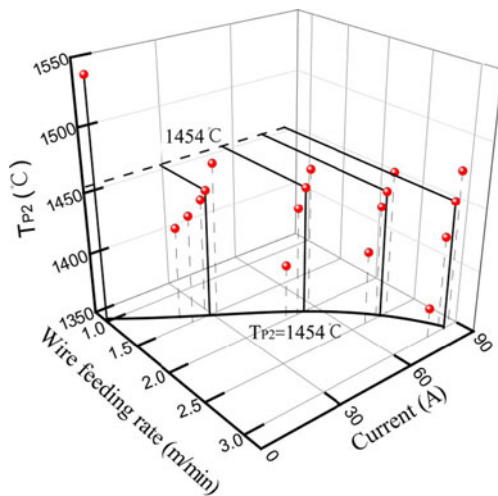


Fig. 14 Influence of wire feeding rate and current on calculated T_{P2} ; ($P=2$ kW)

surface are chosen, the fusing wire transfer behavior is obtained. The bottom surface is the isothermal surface of $T_{P2}=1454$ °C. With welding parameters in the area between the two surfaces, the continuous transfer is obtained, while wire hit transfer below the bottom surface.

The isothermal surfaces of $T_{P1}=1398$ °C and $T_{P2}=1454$ °C can be expressed as Eqs. (8) and (9), respectively, by data fitting. It can be found that the ratio of the square of current and wire feeding rate keeps constant in the isothermal surface of $T_{P1}=1398$ °C. Current and laser power increase with increasing wire feeding rate, and current decreases with decreasing laser power in the isothermal surface of $T_{P2}=1454$ °C. The control principle of the stable wire transfer can be interpreted as two parts: to prevent the wire fusing $I^2/V_f \leq 4512.5$ and to prevent the wire hit: $(I^2 + 4700P - 4292)/V_f \geq 4079.8$.

$$I^2/V_f = 4512.5 \tag{8}$$

$$\frac{I^2}{V_f} + \frac{4700P - 4292}{V_f} = 4079.8 \tag{9}$$

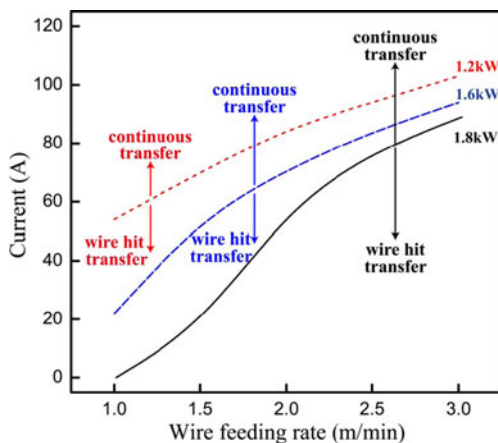


Fig. 15 Isotherms of $T_{P2}=1454$ °C under different laser powers

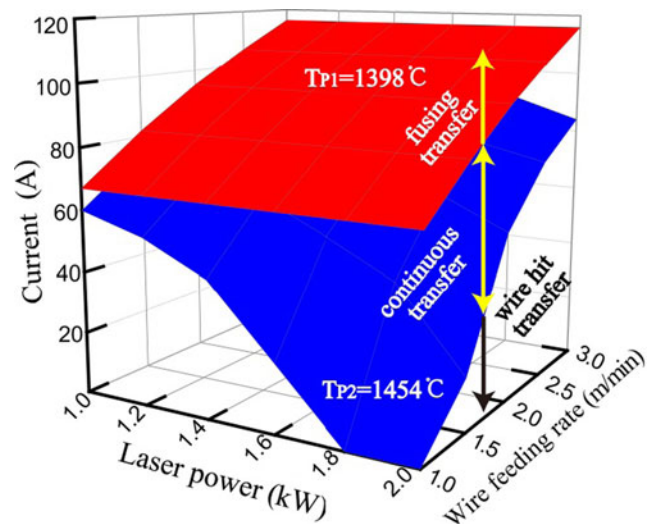


Fig. 16 Window of welding parameters for stable wire transfer

$$Q_R = I^2 \cdot R \cdot t = I^2 \cdot (\rho' \cdot l / S) \cdot \frac{l}{V_f} = (\rho' \cdot l^2 / S) \cdot \frac{I^2}{V_f} \tag{10}$$

According to Figs. 3 and 13, T_{P1} has nothing to do with laser power and is determined by resistance heat. The resistance heat Q_R is expressed as Eq. (10). S is the area of wire cross section; l is the heated length of wire; ρ' is the electrical resistivity of wire. It is found that Q_R is proportion to I^2/V_f with S , l , and ρ' all kept constant. In other words, T_{P1} is determined by I^2/V_f for certain wire. Taking the used wire of 308 L, for example, T_{P1} stays at 1398 °C if the value of I^2/V_f is kept as 4512.5. For any selected wire feeding rate, the maximum current to keep the continuous transfer can be figured out using Eq. (8). If a higher current or a lower wire feeding rate is used, the resistance heat becomes so high that the fusing transfer is obtained.

With controlling resistance heat, the fusing transfer is avoided. The preheated wire feeds inside the molten pool and still needs some conduction heat to melt. The conduction heat from the molten pool is decided by the temperature of the molten pool and the holding time of the wire in the molten pool. The temperature of the molten pool increases with laser power, and the holding time decreases with the wire feeding rate. The total of resistance heat and conduction heat must exceed the energy necessary to melt the wire, which is the physical meaning of Eq. (9). For cold wire without preheating effect, only laser energy is used to melt wire. So laser power must be higher or wire feeding rate must be lower in order to keep the wire melt compared with wire laser welding. Likewise, if the conduction heat is not enough to melt the preheat wire in hot wire laser welding, the wire hit transfer is obtained. The more resistance heat the wire obtains the less laser energy the wire needs to melt, which is beneficial to keep the continuous transfer generally. However, if the resistance heat is too high to make T_{P1} over the solidus, the fusing transfer is unavoidable.

4 Conclusions

The wire transfer behaviors, decided by the wire temperature, are the key factor on the weld formation in hot wire laser welding. The classification and control of the wire transfer behaviors are researched, and the following conclusions are obtained.

The wire transfer behaviors are divided into three types: fusing transfer, continuous transfer, and wire hit transfer. Only the continuous transfer is the stable wire transfer, which is the prerequisite factor for good weld formation.

Wire transfer behaviors are determined by the melting position of hot wire. By defining the characteristic points P1 and P2, temperature criterions of wire transfer behaviors are concluded. For the stable wire transfer, T_{P1} must be lower than the wire solidus and T_{P2} must be higher than the wire liquidus. P1 is outside the molten pool and related to the critical partial melting length, which is decided by the chemical composition and geometry of the used wire regardless of welding parameters. P2 is in the molten pool and located at the end of filler wire, determined mainly by the initial wire length.

Wire temperature is calculated out by numerical simulation. The calculation is in good correspondence with temperature measurement. By comparing calculated T_{P1} and T_{P2} with the temperature criterions, wire transfer behaviors are predicted well under various welding conditions.

The isothermal surfaces of $T_{P1}=1398\text{ }^{\circ}\text{C}$ and $T_{P2}=1454\text{ }^{\circ}\text{C}$ are obtained by calculation with current, wire feeding rate, and laser power as variables. The processing window for the stable wire transfer is obtained, and the control principle for the used wire is concluded as follows: $I^2/V_f \leq 4512.5$; $(I^2 + 4700P - 4292)/V_f \geq 4079.8$. The resistance heat cannot exceed the value which makes the wire tip fuse outside the molten pool, as well as the sum of resistance heat and the conduction heat from the molten pool to wire must exceed the value which makes the wire end melt in time inside the molten pool.

Acknowledgments This research was supported by the National Natural Science Foundation of China (51005125) and National Basic Research Program of China (2011CB013404)

References

1. Salminen AS, Kujanpaa VP, Moisio TJ (1996) Interactions between laser beam and filler metal. *Weld J* 75(1):9–13
2. Sun Z, Salminen AS (1997) Current status of laser welding with wire feed. *Mat Manuf Process* 12(5):759–777
3. Richard P, Martukanitz A (2005) Critical review of laser welding. In *Proceedings of SPIE*. Bellingham, SPIE, 5706: 11–24,
4. Nurminen J, Riihimäki J, Näkki J, Vuoristo P (2006) Comparison of laser cladding with powder and hot and cold wire techniques. In *Proceedings of ICALEO*. Scottsdale, Laser Institute of America: 634–637
5. Nurminen J, Riihimäki J, Näkki J, Vuoristo P (2007) Hot-wire cladding process studies. In *Proceedings of ICALEO*. Orlando, Laser Institute of America: 947–952
6. Liu S, Liu W, Harooni M, Ma J, Kovacevic R (2014) Real-time monitoring of the laser hot-wire cladding of Inconel 625. *Opt Laser Technol* 62:124–134
7. Wen P, Feng ZH, Zheng SQ (2015) Formation quality optimization of laser hot wire cladding for repairing martensite precipitation hardening stainless steel. *Opt Laser Technol* 65:180–188
8. Ohnishi T, Kawahito Y, Mizutani M, Katayama S (2013) Butt welding of thick high strength steel plate with a high power laser and hot wire to improve tolerance to gap variance and control weld metal oxygen content. *Sci Technol Weld Join* 18(4):314–322
9. Phaoniam R, Shinozaki K, Yamamoto M, Kadoi K, Tsuchiya S, Nishijima A (2013) Development of a highly efficient hot-wire laser hybrid process for narrow-gap welding: welding phenomena and their adequate conditions. *Weld World* 57:607–613
10. Jones M, Erikson C, Nowak D (2004) Laser hot wire welding for minimizing defects. In *Proceedings of ICALEO*. Orlando, Laser Institute of America: 1–8
11. Yamamoto M, Shinozaki K, Kadoi K, Inoue T, Fukahori M, Kitahara Y (2011) Development of hot-wire laser welding method for lap joint of steel sheet with wide gap. *Q J Jpn Weld Soc* 29(3): 58–61
12. Kadoi K, Shinozaki K, Yamamoto M, Owaki K, Inose K, Tkayanagi D (2011) Development of high efficiency high quality hot-wire laser fillet welding process. *Q J Jpn Weld Soc* 29(3):62–65
13. Liu W, Ma J, Liu S, Kovacevic R (2015) Experimental and numerical investigation of laser hot wire welding. *Int J Adv Manuf Technol* 78(9-12):1485–1499
14. Liu W, Liu S, Ma J, Kovacevic R (2014) Real-time monitoring of the laser hot-wire welding process. *Opt Laser Technol* 57: 66–76